ARTICLE

Synthesis, Structure, and Characterization of a Microporous Metal-Organic Framework with PtS Topology

Qing-Feng Zhang,[a,b] Jun-Hua Luo,*[b] and Ai-Hua Yuan*[a]

Abstract. The microporous metal-organic framework $Cd_2(ABTC)$-$(H_2O)(DMA)_2 \cdot H_2O \cdot 3DMA$ (**1**) (H_4ABTC = 3,3′,5,5′-azobenzene-tetracarboxylic acid; DMA = N,N'-dimethylacetamide) was prepared by solvothermal reaction and characterized. X-ray structure analysis revealed that compound **1** is a three-dimensional (3D) open framework with 2D channels. The topology is based on a PtS net, constructed of 4-connected rectangular $ABTC^{4-}$ units with 4-connected tetrahedral dinuclear $Cd_2(CO_2)_4(H_2O)(DMA)_2$ secondary building units (SBUs). The solid-state excitation-emission spectra showed that the strongest emission peak is at 403 nm upon excitation at λ = 287 nm.

Introduction

Metal-organic frameworks (MOFs) are one of the most significant breakthroughs in solid-state science, and among many potential applications that may capitalize on these extraordinary properties are hydrogen storage, ion exchange, nonlinear optics (NLO), conductivity, magnetism, chirality, catalysis, luminescence and so on.[1] Up to date, much effort has been devoted into the crystal engineering of MOFs, and in fact a variety of factors, including the solvent system, pH value, template, temperature, stoichiometry, central metal atoms and anions, have been proved to influence the orienting and outcome of these crystallization processes.[2] The prediction and control of these structures is, however, still at a primitive stage. Exploring highly symmetrical multifunctional organic ligands and suitable metal salts in a design strategy to construct MOFs with special topologies (Pt_3O_4, boracites, NbO and PtS nets) is of higher interest, due to the predictability of the resulting networks.[3–6]

Based on above analysis, we used the tetracarboxylate ligand, 3,3′,5,5′-azobenzenetetracarboxylic acid (H_4ABTC),[7] of which several MOFs have already been constructed.[8–13] Herein we report the synthesis, structure and luminescence of the new MOF, $Cd_2(ABTC)(H_2O)(DMA)_2 \cdot H_2O \cdot 3DMA$ (**1**) (DMA = N,N'-dimethylacetamide) with a PtS net. Compound **1** is similar to JUC-63[9] but there exist some differences in the synthesis methods and structural features. Compound **1** was synthesized under solvothermal reaction, whereas JUC-63 was

obtained at room temperature. The structural difference of both compounds may not only be caused by the solvent system but also by the synthesis procedure.

Results and Discussion

Single crystal X-ray diffraction studies revealed that compound **1** crystallizes in the monoclinic $P2_1/c$ space group (Table 1, Table 2), which is different from JUC-63 (orthorhombic system, $Pna2_1$ space group) reported previously[9] and consists of a three-dimensional (3D) open framework.

Table 1. Crystallographic data and structural refinement for compound **1**.

	1
Formula	$C_{36}H_{55}Cd_2N_7O_{15}$
M_r	1050.67
Crystal system	Monoclinic
Space group	$P2_1/c$
a /Å	14.319(3)
b /Å	14.490(3)
c /Å	22.598(5)
α /°	90.00
β /°	98.21(3)
γ /°	90.00
V /Å^3	4640.8(16)
Z	4
$\rho_{calcd.}$ /g·cm^{-3}	1.504
μ /mm^{-1}	0.985
$F(000)$	2144
Total, unique	31677, 9099
Observed [$I > 2\sigma(I)$]	6117
R_{int}	0.0553
GOF on F^2	1.063
R_1, wR_2 [$I > 2\sigma(I)$]	0.0527, 0.1100
R_1, wR_2 (all data)	0.0756, 0.1148
$\Delta\rho_{max}, \Delta\rho_{min}$ /e·Å^{-3}	0.704, –0.985

* Prof. Dr. A.-H. Yuan
  E-Mail: aihuayuan@163.com
* Prof. Dr. J.-H. Luo
  E-Mail: jhluo@fjirsm.ac.cn
[a] School of Biology and Chemical Engineering
  Jiangsu University of Science and Technology
 Zhenjiang 212003, P. R. China
[b] Key Laboratory of Optoelectronic Materials Chemistry and Physics
  Fujian Institute of Research on the Structure of Matter
  Chinese Academy of Sciences
  Fuzhou 350002, P. R. China

**Table 2.** Selected bond lengths /Å and angles /° for compound **1**.

Cd1–O1W	2.230(4)	Cd2–O8^{iii}	2.263(3)
Cd1–O9	2.238(4)	Cd2–O3^{ii}	2.289(4)
Cd1–O1	2.259(3)	Cd2–O5	2.299(3)
Cd1–O4^{ii}	2.287(4)	Cd2–O7^{iii}	2.426(3)
Cd1–O5	2.310(3)	Cd2–O6	2.556(4)
Cd1–O10	2.235(4)	Cd2–O4^{ii}	2.774(4)
Cd2–O2	2.226(3)		
O1W–Cd1–O10	90.48(15)	O4^{ii}–Cd2–O5	77.47(13)
O1W–Cd1–O9	95.07(15)	O2–Cd2–O8^{iii}	98.03(13)
O10–Cd1–O9	89.35(15)	O2–Cd2–O3^{ii}	93.05(14)
O1W–Cd1–O1	87.95(15)	O8^{iii}–Cd2–O3^{ii}	98.12(16)
O10–Cd1–O1	177.55(14)	O2–Cd2–O5	101.38(13)
O9–Cd1–O1	88.91(14)	O8^{iii}–Cd2–O5	136.59(13)
O1W–Cd1–O4^{ii}	93.35(16)	O3^{ii}–Cd2–O5	118.99(14)
O10–Cd1–O4^{ii}	87.55(14)	O2–Cd2–O7^{iii}	153.19(12)
O9–Cd1–O4^{ii}	171.05(14)	O8^{iii}–Cd2–O7^{iii}	55.17(12)
O1–Cd1–O4^{ii}	94.42(14)	O3^{ii}–Cd2–O7^{iii}	91.97(15)
O1W–Cd1–O5	170.09(15)	O5–Cd2–O7^{iii}	99.11(12)
O10–Cd1–O5	92.83(14)	O2–Cd2–O6	88.09(13)
O9–Cd1–O5	94.31(12)	O8^{iii}–Cd2–O6	89.35(14)
O1–Cd1–O5	89.03(13)	O3^{ii}–Cd2–O6	172.21(14)
O4^{ii}–Cd1–O5	77.47(13)	O5–Cd2–O6	53.27(11)
O1W–Cd1–O10	90.48(15)	O7^{iii}–Cd2–O6	90.46(14)
O1W–Cd1–O9	95.07(15)	O4^{ii}–Cd2–O5	77.47(13)
O10–Cd1–O9	89.35(15)	O2–Cd2–O8^{iii}	98.03(13)
O4^{ii}–Cd2–O2	105.02(13)	O4^{ii}–Cd2–O6	121.59(13)
O4^{ii}–Cd2–O3^{ii}	50.71(14)	O4^{ii}–Cd2–O7^{iii}	98.50(13)
O4^{ii}–Cd2–O5	68.33(12)	O4^{ii}–Cd2–O8^{iii}	141.32(13)

Symmetry codes: (ii) $x + 2$, $y + 1/2$, $-z + 3/2$; (iii) $-x + 1$, $y + 1/2$, $-z + 3/2$.

The asymmetric unit of compound **1** contains two Cd^{2+} ions, one crystallographically equivalent ABTC^{4-} ligand, one coordinated H$_2$O molecule, two coordinated DMA ligands, and crystallized H$_2$O and DMA molecules (Figure 1). The central Cd1 atom adopts a distorted octahedral coordination arrangement with six oxygen atoms from three different ABTC^{4-} ligands (O1, O4^{ii}, and O5), one H$_2$O molecule (O1W) and two DMA molecules (O9, O10). The central Cd2 atom is coordinated by seven oxygen atoms (O2, O3^{ii}, O4^{ii}, O5, O6, O7^{iii}, and O8^{iii}) from four different ABTC^{4-} ligands to form distorted capped octahedron coordination arrangement, which is different from the six-coordinate Cd^{II} atoms in JUC-63. The central Cd1 and Cd2 atoms are bridged through oxygen atoms from carboxylate groups, and the coordination mode of H$_4$ABTC in compound **1** is shown in Scheme 1. The ABTC^{4-}
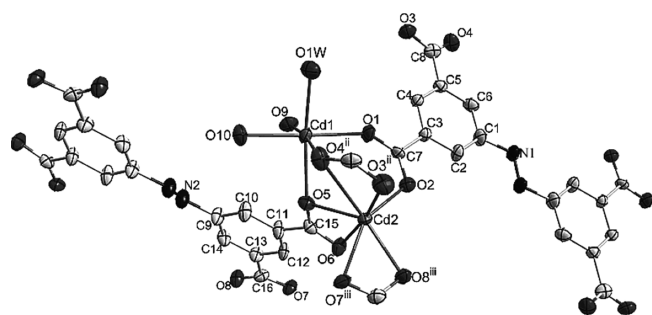
Figure 1. ORTEP diagram of compound **1**. All hydrogen atoms, guest H$_2$O, and DMA molecules are omitted for clarity. Symmetry codes: (ii) $x + 2$, $y + 1/2$, $-z + 3/2$; (iii) $-x + 1$, $y + 1/2$, $-z + 3/2$.

ligands chelate to Cd^{II} atoms and the carboxylate groups are all deprotonated. The differences between compound **1** and JUC-63 in the central Cd^{II} coordination environments are probably that the three coordinated DMF molecules of a central Cd^{II} atom in JUC-63 are substituted by one H$_2$O molecules and two DMA molecules in compound **1**. The DMA molecule is larger than DMF molecule in the space size, which makes one carboxylate oxygen atom moving closely to another Cd^{II} atom, and there exits an intermediate interaction between them with a bond length of 2.771(6) Å.
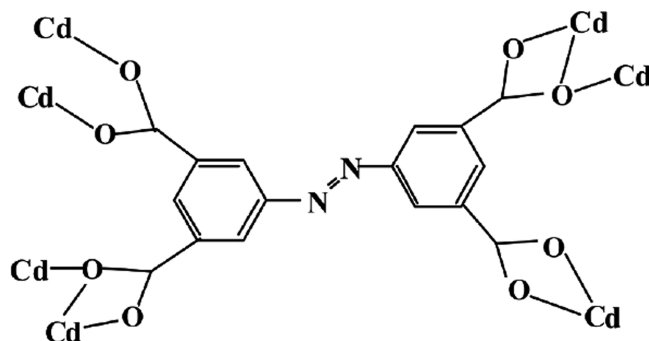

Scheme 1. Representation of the coordination mode of H$_4$ABTC in compound **1**.

The crystallographically distinct Cd^{II} atoms are bridged to construct tetrahedral secondary building units (SBUs) that is defined by the carboxylate carbon atoms (Figure 2a). Each ABTC^{4-} unit coordinating to four tetrahedral SBUs can act as rectangular SBUs, which is also defined by the carboxylate carbon atoms (Figure 2b). The dihedral angles between these rectangular SBUs in the structure range from 0.41° to 9.38°, which is apparently induced by their coordinated forms. The tetrahedral SBUs and rectangular SBUs are interconnected by distorted ABTC^{4-} ligands, thereby generating a 3D extended network. The cubic cage is defined by six ABTC^{4-} SBUs with pore diameter of about 10.5 Å (Figure 2c). When the van der
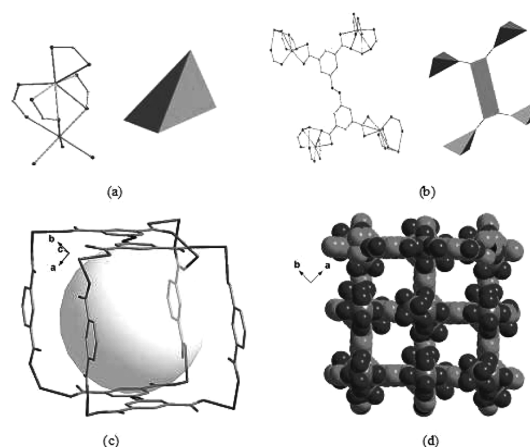
Figure 2. The single-crystal X-ray structure of compound **1**. (a) Two central cadmium atoms, which can be viewed as a 4-connected node; (b) the organic linker ABTC^{4-} unit, which can be act as a 4-connected node (c) the cage in compound **1** is defined by six organic SBUs with a pore diameter of about 10.5 Å; (d) infinite 3D framework with 2D channels.

Waals radii of the atoms are taken into account, these channels are about 10.0 Å × 10.0 Å (Figure 2d), in which the vacancies are filled by one terminal H_2O molecule, two terminal DMA ligands, and one H_2O molecule, three DMA guest molecules per formula unit. Without guest molecules, the effective free volume of compound **1** is calculated by PLATON analysis to be ca. 35.2 % of the crystal volume (1633.6 Å^3 of the 4640.8 Å^3 unit cell volume).[14] Removing the coordinated H_2O and DMA molecules, the effective free volume reaches ca. 53.1 % of the crystal volume (2464.3 Å^3 of the 4640.8 Å^3 unit cell volume) and the calculated density of the framework is 1.504 g·cm^{-3}.

A better insight into the nature of the involuted framework of compound **1** can be achieved by the application of a topological approach, i.e., reducing multidimensional structures to simple node-and-connection nets. As discussed above, both the tetrahedral SBU (SBU1) and rectangular SBU (SBU2) are defined as 4-connected nodes. On the basis of the simplification principle, the resulting structure of compound **1** is a bimodal (4,4)-connected net with two 4-connected nodes and its Schläfli symbol is $(4^2·8^4)$, where the SBU1 with the extended point symbol: [4·4·8(7)·8(7)·8(7)·8(7)] node, and the SBU2 has the extended point symbol: [4·4·8(2)·8(2)·8(8)·8(8)] node,[15] therefore the topological type of compound **1** is bimodal PtS (Figure 3).
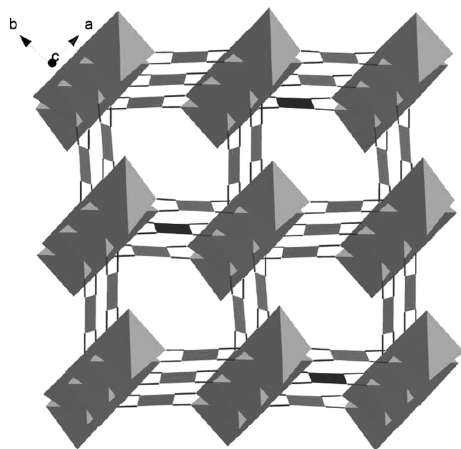

Figure 3. Schematic illustration of the PtS topological network for compound **1**. Light gray: 4-connected tetrahedral SBUs; dark gray: 4-connected rectangular SBUs.

TG analysis of compound **1** was performed on polycrystalline sample in a nitrogen atmosphere (Figure 4). The TG curve showed that the weight loss of 1.83 % during the first step between 30 and 100 °C corresponds to the loss of one guest H_2O molecule (calculated 1.71 %). This step is followed by an additional 26.79 % weight loss from 100 to 255 °C, corresponding to the loss of one coordinated H_2O molecule and three guest DMA molecules (calculated 26.59 %). The following weight loss at higher temperatures corresponds to the loss of two coordination DMA molecules, together decomposition of the host framework.
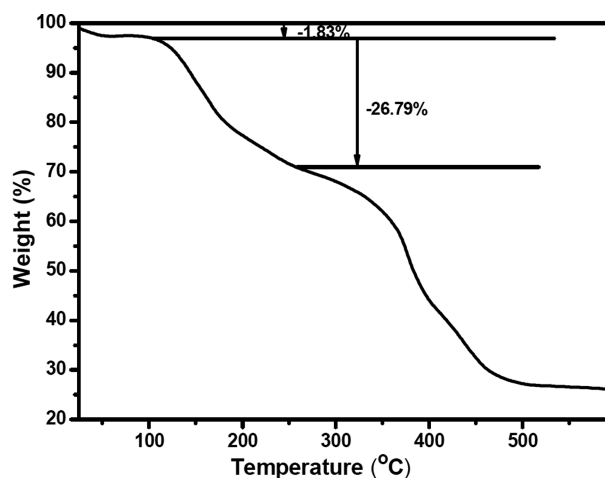
Figure 4. TG curve of compound **1**.

The solid-state excitation-emission spectra of the free H_4ABTC ligand and compound **1** were studied at room temperature, as depicted in Figure 5. The strongest emission peak for the free H_4ABTC ligand is at 378 nm with the excitation peak at 277 nm, which may be attributed to the $\pi^*\rightarrow n$ or $\pi^*\rightarrow\pi$ internal transitions of the ligand.[16] Compared with the free H_4ABTC, the strongest excitation peak for compound **1** is at 287 nm. Its emission spectra show obvious red-shift and exhibit the strong peak at 403 nm. The emission peak of compound **1** can be assigned to the ligand-to-metal charge-transfer (LMCT) band.[17] The enhancement of the emissions for compound **1** compared with those of the free ligand may be ascribed to the increase of the ligand conformational rigidity due to their coordination to Cd^{II} ions, which might result in a decrease in the non-radiative decay of intra-ligand excited states.[18] We found that the solid state emission ($\lambda = 403$ nm) of compound **1** was similar to that (402 nm) of JUC-63. Compound **1** might be treated as a candidate for the potential luminescent material.[9,19,20]
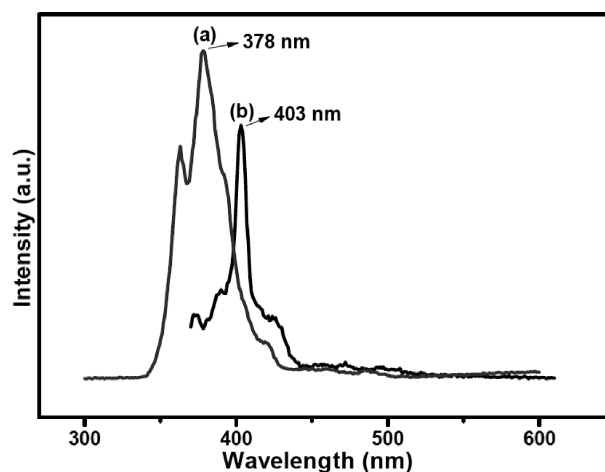
Figure 5. Solid-state emission spectra at room temperature of the free H_4ABTC ligand excited at 277 nm (a) and compound **1** excited at 287 nm (b).

Conclusions

We have synthesized and characterized the new 3D microporous MOF, $Cd_2(ABTC)(H_2O)(DMA)_2 \cdot H_2O \cdot 3DMA$ (**1**). Single crystal X-ray diffraction analysis reveals that compound **1** is a 3D open framework with PtS-type topology with 2D channels. Compound **1** exhibits strong main emission peak at 403 nm at room temperature in the solid state. The successful preparation of compound **1** containing rigid tetracarboxylate ligands may provide a useful route for the design and synthesis of PtS-type MOFs.

Experimental Section

Materials and General Methods: All reagents, unless otherwise stated, were obtained from commercial sources and were used without further purification. Elemental analyses for C, H, and N were performed with an Elemental Vario ELIII elemental analyzer. Infrared spectra as KBr pellets were recorded with a Perkin-Elemer Spectrum One FT-IR spectrophotometer from 4000 to 450 cm^{-1}. The emission/excitation spectra were recorded with an Edinburgh Instrument FL920 fluorescence spectrophotometer with single crystal samples being used in photoluminescence analysis.

Synthesis: A mixture of H$_4$ABTC (8.95 mg, 0.025 mmol), Cd(NO$_3$)$_2 \cdot 4H_2O$ (18.5 mg, 0.06 mmol), L-glutamic acid (14.7 mg, 0.1 mmol), 0.5 mL H$_2$O, a few drops of HNO$_3$ (2.5 M), and 2 mL DMA was stirred for 20 min at room temperature. The solution was heated in a Teflon-lined stainless-steel vessel at 85 °C for 2 d, and cooled to room temperature at the rate of 5 °C·h^{-1}. The yellow block-shaped product **1** was collected by filtration and washed with DMA. Yield (based on the Cd salt): 36 %. The products are insoluble in water and common organic solvents. Elemental analysis for C$_{36}$H$_{55}$N$_7$O$_{15}$Cd$_2$: calcd. C 41.15, H 5.28, N 9.33 %; found C 42.38, H 5.19, N 9.42 %. **IR** (KBr): $\tilde{v}$ = 3381 (w), 2934 (w), 1640 (vs), 1569 (m), 1438 (m), 1373 (s), 1236 (m), 1116 (s), 1060 (w), 1014 (m), 963 (w), 924 (w), 847 (w), 776 (s), 726 (s), 616 (m), 513 (w) cm^{-1}. It should be noted that the absence of the L-glutamic acid had not lead to the isolation of any crystals.

X-ray Crystallographic Analysis: Single-crystal structure measurements for compound **1** were performed with a Saturn 724 CCD diffractometer using graphite-monochromatized Mo-K_α radiation (λ = 0.71073 Å) at room temperature using ω-scan technique. Diffraction data analysis and reduction were performed within SMART, SAINT, and XPREP.[21] Correction for Lorentz, polarization and absorption effects were performed within SADABS.[22] Structures were solved using Patterson method within SHELXS-97 and refined using SHELXL-97.[23–25] Anisotropic thermal parameters were assigned to all non-hydrogen atoms. The hydrogen atoms bound to water molecules were located from difference Fourier maps and refined as riding mode.

Crystallographic data (excluding structure factors) for the structure in this paper have been deposited with the Cambridge Crystallographic Data Centre, CCDC, 12 Union Road, Cambridge CB21EZ, UK. Copies of the data can be obtained free of charge on quoting the depository number CCDC-806577 (Fax: +44-1223-336-033; E-Mail: deposit@ccdc.cam.ac.uk, http://www.ccdc.cam.ac.uk)

Acknowledgements

References

[1] H. C. Zhou, J. R. Long, O. M. Yaghi, *Chem. Rev.* **2012**, *112*, 673–674.

[2] X. Y. Duan, Y. Z. Li, F. M. Wang, C. S. Lu, Q. J. Meng, Q. X. Zhang, *Inorg. Chem. Commun.* **2010**, *13*, 1239–1243.

[3] B. P. Johnson, F. Dielmann, G. Balázs, M. Sierka, M. Scheer, *Angew. Chem. Int. Ed.* **2006**, *45*, 2473–2475.

[4] X. Lin, J. Jia, X. Zhao, K. M. Thomas, A. J. Blake, G. S. Walker, N. R. Champness, P. Hubberstey, M. Schröder, *Angew. Chem. Int. Ed.* **2006**, *45*, 7358–7364.

[5] A. H. Yuan, R. Q. Lu, H. Zhou, Y. Y. Chen, Y. Z. Li, *CrystEngComm* **2010**, *12*, 1382–1384.

[6] X. Chen, H. Zhou, Y. Y. Chen, A. H. Yuan, *CrystEngComm* **2011**, *13*, 5666–5669.

[7] S. Wang, X. Wang, L. Li, R. C. Advincula, *J. Org. Chem.* **2004**, *69*, 9073–9084.

[8] Y. L. Liu, J. F. Eubank, A. J. Cairns, J. Eckert, V. C. Kravtsov, R. Luebke, M. Eddaoudi, *Angew. Chem. Int. Ed.* **2007**, *46*, 3278–3283.

[9] M. Xue, G. S. Zhu, Y. X. Li, X. J. Zhao, Z. Jin, E. H. Kang, S. L. Qiu, *Cryst. Growth Des.* **2008**, *8*, 2478–2483.

[10] W. L. Liu, L. H. Ye, X. F. Liu, L. M. Yuan, J. X. Jiang, C. G. Yan, *CrystEngComm* **2008**, *10*, 1395–1403.

[11] Y. G. Lee, H. R. Moon, Y. E. Cheon, M. P. Suh, *Angew. Chem. Int. Ed.* **2008**, *47*, 7741–7745.

[12] X. S. Wang, S. Q. Ma, K. Rauch, J. M. Simmons, D. Q. Yuan, X. P. Wang, T. Yildirim, W. C. Cole, H. C. Zhou, *Chem. Mater.* **2008**, *20*, 3145–3152.

[13] A. J. Cairns, J. A. Perman, L. Wijtas, V. C. Kravtsov, M. H. Alkordi, M. Eddaoudi, M. J. Zaworotko, *J. Am. Chem. Soc.* **2008**, *130*, 1560–1561.

[14] A. L. Spek, *J. Appl. Crystallogr.* **2003**, *36*, 7–13.

[15] V. A. Blatov, M. V. Peaskov, *Acta Crystallogr., Sect. B* **2006**, *62*, 457–466; V. A. Blatov, *Ac. Pavlov St. 1*, 443001, Samara, Russia, TOPOS 4.0, http://www.topos.ssu.samara.ru/, accessed May **2009**.

[16] Y. Y. Liu, J. C. Ma, Y. P. Xie, J. F. Ma, *J. Coord. Chem.* **2008**, *61*, 3450–3457.

[17] Q. R. Fang, G. S. Zhu, Z. Jin, Y. Y. Ji, J. W. Ye, M. Xue, H. Yang, S. L. Qiu, *Angew. Chem. Int. Ed.* **2007**, *46*, 6638–6642.

[18] H. Yersin, A. Vogler, Eds., *Photochemistry and Photophysics of Coordination Compounds*, Springer-Verlag, Berlin, **1987**.

[19] X. L. Wang, C. Qin, N. Hao, C. W. Hu, L. Xu, *Inorg. Chem.* **2004**, *43*, 1850–1856.

[20] Q. R. Fang, G. S. Zhu, M. Xue, J. Y. Sun, X. T. Li, S. L. Qiu, *Inorg. Chem.* **2006**, *45*, 3582–3587.

[21] Bruker; *SMART*, *SAINT* and *XPREP*: Area Detector Control and Data Integration and Reduction Software, Bruker Analytical X-ray Instruments Inc., Madison, Wisconsin, USA, **1995**.

[22] G. M. Sheldrick, *SADABS*: Empirical Absorption and Correction Software, Göttingen, Göttingen, Germany, **1996**.

[23] G. M. Sheldrick, *SHELXS-97*. Program for X-ray Crystal Structure Determination; Göttingen, Germany, **1997**.

[24] G. M. Sheldrick, *SHELXL-97*. Program for X-ray Crystal Structure Determination; University of Göttingen, Göttingen, Germany, **1997**.

[25] G. M. Sheldrick, *Acta Crystallogr., Sect. A* **2008**, *64*, 112–122.